

An empiric method for separation of extra- and intra-cellular signal in mouse spinal cord for q-space imaging

Henry H. Ong¹, and Felix W. Wehrli¹

¹Laboratory for Structural NMR Imaging, Department of Radiology, University of Pennsylvania School of Medicine, Philadelphia, PA, United States

Introduction

Q-space imaging^{1,2} offers potential for non-destructively assessing white matter (WM) micro-architecture by exploiting the regularity of molecular diffusion barriers from axon membranes and myelin sheaths³. The q-space signal decay ($E(q)$) and its Fourier transform (FT), the displacement probability density function (d-PDF), both contain axon structure information such as mean axon diameter (MAD) and intracellular volume fraction (ICF)⁴. However, the $E(q)$ and d-PDF contain signal from both extra- and intra-cellular spaces (ECS and ICS, respectively). Accurate WM architecture assessment would require separation of both signals. Current approaches rely on numeric Laplace inversion⁵, which is a difficult ill-posed problem, or fitting with a model⁶, which requires *a priori* assumptions that may not be valid. Here, we developed an empiric method that separates ECS and ICS signals to circumvent these problems. This method is based on a previous method to empirically estimate ICS fraction⁷ in which multiple $E(q)$ curves are obtained at the same q-values ($q = (2\pi)^{-1}\gamma G\delta$, G = gradient amplitude, and δ = gradient duration) while varying δ . Diffusion in the ICS and ECS are expected to be restricted and Gaussian, respectively⁶, and have different dependences on δ ⁸. Gaussian diffusion is unaffected by changes in δ , while restricted diffusion exhibits less signal decay with increasing δ . The ECS and ICS signals can then be separated by a comparison of the $E(q)$ curves. We validate this new method by measuring the MAD of WM tracts in healthy mouse spinal cords (SC), which have a simple WM structure to facilitate interpretation, and compare the results with histology.

Methods

Previously published data⁴ was reanalyzed here and a brief summary of the methodology is given below. Five SC sections were dissected from perfusion-fixed adult female C57 BL/6 mice. Experiments were performed with a custom-built 50T/m z-gradient/RF coil set interfaced to a 9.4T micro-imaging system (Bruker DMX 400). A diffusion-weighted stimulated-echo sequence was used: 64×64 , FOV/THK = $4/1\text{mm}$, and $TE/\Delta\delta = 17.4/10/0.4\text{ms}$. Two experiments were run with $\delta = 0.4$ and 5ms yielding echo attenuations $E(\delta=0.4\text{ms})$ and $E(\delta=5\text{ms})$, respectively. The diffusion gradient was applied perpendicular to the SC long axis in 64 increments of q ($q_{\text{max}} = 0.82\ \mu\text{m}^{-1}$). Q-space echo attenuations were obtained for each pixel and averaged over ROIs selected within seven WM tracts (Fig. 1).

As described in [7], the signal attenuation value at which $E(\delta=0.4\text{ms})$ and $E(\delta=5\text{ms})$ begin to deviate from each other, P_d , provides a relaxation-weighted estimate of ICF, which was confirmed with histology in [4]. As P_d accurately estimates ICF, it follows that the echo attenuation before and after P_d must arise from the ECS and ICS signals, respectively. Therefore, P_d can be used to empirically divide $E(q)$ into ECS and ICS parts. The FT of the subdivided $E(q)$ would give the ECS and ICS d-PDFs without any modeling or assumptions of the peak shape. $E(\delta=0.4\text{ms})$ was used to calculate the ECS and ICS d-PDFs. The full-width-at-half-maximum (FWHM) of the ICS d-PDF would then be an estimate of MAD and is compared with histology. Due to the finite maximum q-value possible in experiments, the subdivision of the echo attenuation will reduce the displacement resolution of the ECS and ICS d-PDFs, which may lead to inaccuracies in FWHM measurements. In order to correct this, a non-linear interpolation method similar to subvoxel processing⁹ was used to improve the displacement resolution.

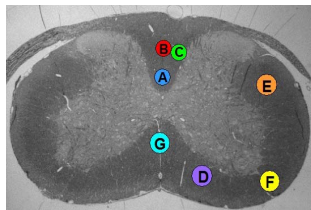


Figure 1. Optical image of SC section showing WM tract locations: A) dorsal corticospinal (dCST), B) gracilis (FG), C) cuneatus (FC), D) rubrospinal (RST), E) spinothalamic (STT), F) reticulospinal (ReST), G) vestibulospinal (VST).

Results and Discussion

Fig. 2a shows examples of measured overall d-PDF with empirically separated ECS and ICS d-PDFs. Note the fewer number of points that describe the ECS d-PDF due to the coarser displacement resolution. Fig. 2b shows plots of ECS and ICS d-PDF FWHMs vs histologic MAD with equations for lines of best fit and R^2 . Each point is a mean value for a specific WM tract that was averaged over all five specimens. The FWHMs of the overall and ICS d-PDF show excellent correlation with histologic MAD. The overall d-PDF has a y-intercept of 0.25, which is in agreement with the observation that the overall PDF FWHM overestimated MAD by $\sim 20\%$ ⁴. The ICS d-PDF has a reduced y-intercept that suggests that the separation of the ECS and ICS signals improved the estimate of MAD. A Bland-Altman analysis confirmed that the ICS d-PDF FWHM accurately estimates MAD. The ECS d-PDF FWHM also showed significant positive correlation with MAD. This is in agreement with previous reports that ECS displacement is correlated with axon density as smaller MAD leads to increased axon packing and therefore tortuosity¹⁰. Importantly, this correlation was not observed when using a two-compartment model to separate ECS and ICS d-PDFs⁴, which may have resulted from inaccuracies in the model.

It should be noted that the data was acquired under ideal conditions ($\delta \ll \Delta$, displacement resolution = $0.6\ \mu\text{m}$) using custom hardware. While theory predicts the possibility of using this method with commercial gradients, further study is needed to validate this method under non-ideal conditions.

Conclusion

This work demonstrates the feasibility of an empiric method to separate ECS and ICS signals for q-space imaging. The results show that under ideal experimental conditions this method can accurately characterize diffusion in the ECS and ICS of WM in SC.

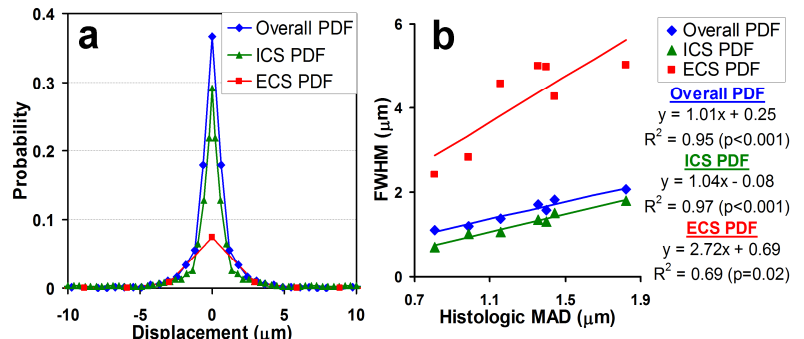


Fig. 2. (a) Overall, ECS, and ICS d-PDFs from the FG tract in a single specimen. (b) Plots of FWHM of overall, ECS and ICS d-PDFs vs histologic MAD with lines of best fit.

References: 1. Callaghan, P.T., *Principles of NMR Microscopy*, Oxford University Press (1991). 2. Cohen, Y., et al., *NMR Biomed*, **15**:516 (2002). 3. Beaulieu, C., *NMR Biomed*, **15**:435 (2002). 4. Ong, H.H., *Neuroimage*, **51**:1360 (2010). 5. Peled S., et al., *MRM*, **42**:911 (1999). 6. Assaf Y., et al., *MRM*, **52**:965 (2002). 7. Malmberg C., et al., *JMR*, **180**:280 (2006). 8. Mitra P.P., et al., *JMR A*, **113**:94 (1995). 9. Hwang, S.N. and F.W. Wehrli, *MRM*, **47**:948 (2002). 10. Schwartz, E.D., et al., *Neuroreport*, **16**:73 (2005).

Acknowledgements: NIH grant R21 EB003951